

Investigation of Some Hard Coatings Synthesized by Ion Beam Assisted Deposition*

Jian-Li He, Wen-Zhi Li, Xiao-Ming He and Chang-Hong Liu
Department of Materials Science and Engineering, Tsinghua University,
Beijing, 100084, China

ABSTRACT

Ion beam assisted deposition (IBAD) technique was used to synthesize hard coatings including diamond-like carbon (DLC), carbon nitride (CN) and metal-ceramic multilayered films. It was found that DLC films formed at low energy ion bombardment possess more SP^3 bonds and much higher hardness. The films exhibited an excellent wear resistance. Nanometer multilayered Fe/TiC films was deposited by ion beam sputtering. The structure and properties were strongly dependent on the thickness of the individual layers and modulation wave length. It was disclosed that both hardness and toughness of the films could be enhanced by adjusting the deposition parameters. The CN films synthesized by IBAD method consisted of tiny crystallites dispersed in amorphous matrix, which were identified by electron diffraction pattern to be β - C_3N_4 .

1. INTRODUCTION

Ion beam assisted deposition (IBAD) is a combination of ion implantation and physical vapour deposition (PVD). Namely it is a procedure in which energetic ions are employed to bombard the growing film. The energy of bombarding ions ranged from several ten electron volts to about one hundred kilo-electron volts. The selection of ion species depends on the materials to be synthesized. The bombardment of energetic ions provides much more energy than in a conventional vapour deposition. The bombardment can cause atomic mixing at the interface as well. For this reason, the adhesion of film to substrate is greatly enhanced. So IBAD offers a possible access to the modification of engineering materials such as bearing steel at nearly room temperature. Additionally, in IBAD process, parameters are easy to control. This is of great advantage especially for fundamental study of thin film materials. Briefly, IBAD offers a novel technique for both scientific research and technological applications.

Hard coatings have wide-ranging applications for wear-resistant and protective purpose in many industry fields, such as machining tools, precision moving components, etc. The hard coatings over the surface can remarkably enhance the wear resistance of a component. As a result, its dimensional precision can be greatly improved and so do its serving life. The technical demands render hard-coating synthesis to be a very active field for decades. Many techniques have been employed to produce hard materials, such as refractory metallic carbide, nitride, boride, DLC, etc. Some of them have been commercially used, and others are still in the stage of laboratory.

2. EXPERIMENTAL

A schematic diagram of the IBAD system used in the present study is shown in Fig. 1. It is equipped with four Kaufman ion sources. 4 and 5 are focused ion sources with a current of

*The project was supported by Ford, NSFC No 09415105, and 863 committee.

100~150mA, specially designed for sputtering deposition and usually operated at the voltage of 2~4KV. 7 and 8 are two bombarding ion sources. The former works in the high energy range 3~40KeV, while the latter in the low energy range 50~1500eV. 6 represents two rotatable, water-cooled target holders. Four different targets can be set on each one at the same time, which makes it simple and easy to change material during the film deposition. The specimen holder 2 can be either water-cooled or heated by a tungsten filament up to 600°C. The vacuum chamber made of stainless steel is about 700mm in diameter and 800mm long. The base pressure can be evacuated up to 2×10^{-4} Pa by an oil diffusion pump system.

Such an IBAD system proved to be well operated and quite versatile. It offers a great number of possibilities of film composition (from single element film to various alloys and compounds), coupled with different structures. In this paper, we applied IBAD technique to the investigation of three representative hard coatings, e.g. DLC, β -C₃N₄ and nanometer multi-layered Fe/TiC. Both their structures and properties were investigated. The relation of structures and properties to deposition parameters was highlighted. Prior to deposition, substrates were usually cleaned by low energy ion sputtering. Subsequently, high energy ion bombardment was carried out to create an atomic intermixed layer to enhance the adhesion. The parameters of film synthesis will be described in detail in Section 3.

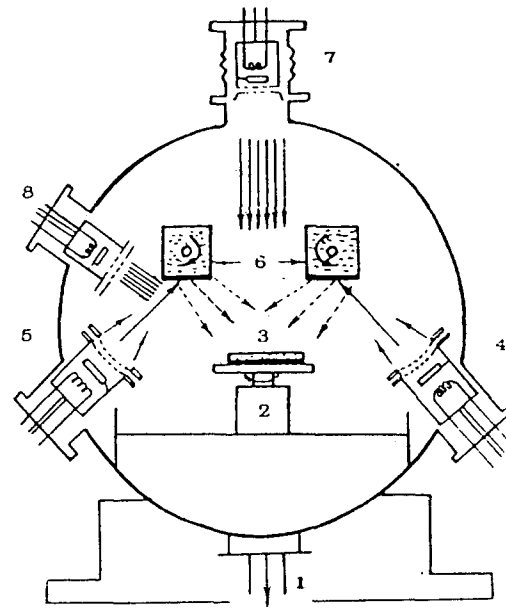


Figure 1. Schematic diagram of IBAD system
 1. To diffusion pump 2. specimen holder 3. sample 4, 5. sputtering ion source 6. target holders 7. high-energy bombardment ion source 8. low-energy bombardment ion source

3. RESULTS AND DISCUSSION

3.1 Diamond-like carbon (DLC)

Diamond-like carbon exhibits many extreme characteristics, such as high hardness, low friction, high thermal conductivity, chemical inertness, etc. These properties have brought it into the foreground of many research programs. Especially due to its superhardness, DLC has elicited considerable attention as wear-resistant films.

DLC films were synthesized by sputtering a pure graphite target with a beam of argon ions, while another ion beam was used to bombard the growing films simultaneously. To investigate the effect of bombardment on the structure and properties of DLC, species of Ar, Ne, N₂, CH₄ at an energy of 100eV~ 25KeV were used. The growth rate was typically 0.8Å/S.

3.1.1 Structure of DLC

The DLC films obtained in our experiment were basically amorphous. The amorphous structure was probably due to the rapid quenching of thermal spikes and the collapse of pressure spikes created by the energetic particles^[1]. However, selected area electron diffraction (SAD) showed that when the bombardment energy was in the range of 200~400eV, there were many diamond crystallites dispersed in the amorphous carbon



Figure 2. SAD pattern of DLC film

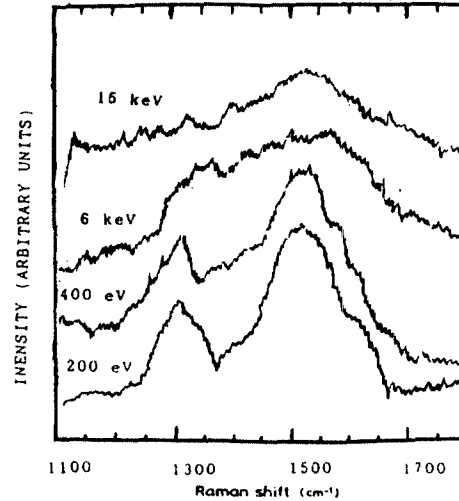


Figure 3. Raman spectra of DLC films

matrix. The SAD pattern of DLC film synthesized under a Ne^+ bombardment of 200eV and $0.19\text{mA}/\text{cm}^2$ is showed in Fig 2. The SAD pattern was identified as that of diamond with: $d(110)=2.57\text{\AA}$, $d(200)=1.83\text{\AA}$, $d(220)=1.29\text{\AA}$, $d(311)=1.12\text{\AA}$, $d(400)=0.92\text{\AA}$. The discrepancy to the standard interplanar spacings was slight. Such diamond crystallites were hardly found in films deposited with high energy bombardment. This somewhat indicates that low energy bombardment is favourable to the formation of diamond phase.

The C-C bonds in DLC films were studied by Raman spectroscopy. Figure 3 shows the spectra of DLC films deposited with various bombarding energy of CH_4 . It is clear that by decreasing the bombarding energy of CH_4 , the Raman spectra gradually changes from a single broad peak at about $1400\sim 1550\text{cm}^{-1}$ to two separated peaks set at about $1500\sim 1550\text{cm}^{-1}$ and about 1300cm^{-1} . The peak at about 1300cm^{-1} represents the diamond characters of the film^[2]. This shows that DLC films deposited at low energy bombardment have more sp^3 bonds. IR spectra and XPS were also employed to determine the bonds in DLC films. A similar conclusion was reached.

3.1.2 Hardness of DLC films

The hardness of DLC films synthesized under various conditions are summarized in table 1. Hardness test was conducted with a Knoop's indenter. Two conclusions can be drawn from the hardness data. First, when the bombarding energy falls into the range of 3Kev~25Kev, the hardness of the films is not very high and insensitive to the bombarding energy. Second, in the range of low bombarding energy, the hardness is quite high. Especially at the bombarding energy of 200eV, the hardness is always higher than $4000\text{Kg}/\text{mm}^2$. The hardness seems to be independent of the bombarding species. The fact that low energy bombardment leads to higher hardness is consistent with the abundant SP^3 bonds.

Table 1. Hardness of DLC films

Bombardment Energy(eV)	200				300	400	500	6K	10K	15K	25K
Bombardment Species	CH_4	CH_4+Ne (1:1)	$\text{CH}_4+\text{Ne}+\text{Ar}$ (2:1:1)	Ne	CH_4						
Hardness Hk (Kg/mm^2)	5100*	4540	4300	4010	3250*	3500	2700	1630	2180	1560	1600

* The load is 20g

3.1.4 Tribological properties of DLC

DLC films for tribological investigation were synthesized on AISI 52100 steel. The films were deposited about $1\mu\text{m}$ thick. In all cases they proved to be highly adherent. The tribological properties of the DLC films under loads of 2~15N were systematically investigated and reported previously.^[3] Here, we highlight DLC's tribological behaviour in ball-on-disk test under high loads of 30~120N.

DLC films exhibit quite low coefficient of friction even in the case of high load. Fig.4 illustrates the friction coefficient under various loads as a function of sliding distance. The film was synthesized under CH_4 bombardment at an energy of 200eV. As can be seen, when the load is increased from 30N to 120N, the friction coefficient does not experience significant change. It maintains at an approximate constant of 0.05, which is much lower than 0.75 — the self-friction coefficient of AISI 52100 steel.

Wear rate of DLC films was found to be $3.42 \times 10^{-6} \text{mm}^3/\text{m}$, which was only one percent of the wear rate of AISI 52100 steel. There is no doubt that the tribological performance of DLC film is much better than that of AISI 52100 steel. What warrant considerable attention is the load of 120N corresponds to a contact stress of about 3.2GPa, which is close to that in industrial bearing service. This confirmed the possibility of industrial application of DLC films serving as anti-wear coatings. A comment should be made here is that all these data were obtained in unlubricated sliding. The magnitude of wear would decrease significantly in lubricated condition^[4].

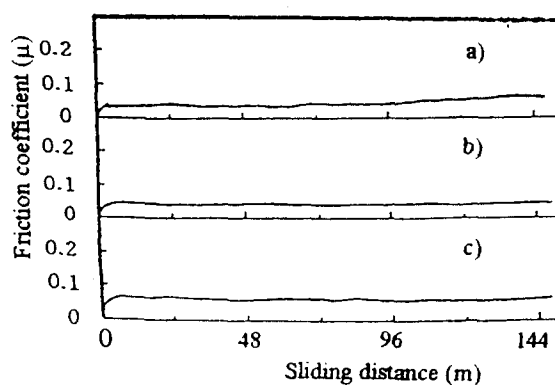


Figure 4. Friction coefficient vs sliding distance under a load of a) 30N b) 50N c) 120N

3.2 Fe/TiC multilayered films

Multilayer materials have been considered to be of great importance for both scientific study and technological applications. Especially when the individual layer thickness is on the nanometer scale they exhibit many intriguing properties of magnetic, electronics, optics, mechanics, etc^[5]. TiC is well known for its high hardness. But it is fragile. We want to see what would happen if TiC and a soft material, such as Fe, are combined into multilayered structure.

Fe/TiC multilayers were prepared by alternately depositing TiC and Fe in the IBA system described in section 2. The Fe layers were produced by sputtering an iron target. The TiC layers were synthesized by sputtering a composite target of graphite and titanium. The ratio of Ti to C in the composite target was adjusted to form stoichiometric TiC, which was confirmed by XPS, AES and XRD. The alternate deposition was accomplished by rotating the four-fold target holder. The deposition rate was $0.5\text{\AA}/\text{s}$ for TiC and $2\text{\AA}/\text{s}$ for Fe. Individual layer thickness varied from 1~12nm for Fe and 2~10nm for TiC. The working pressure in the chamber was $7 \times 10^{-3} \text{Pa}$. The substrates were water-cooled to maintain at room temperature.

3.2.1 Structure of multilayer Fe/TiC films

Layered structure in the deposited films was determined by low angle X-ray

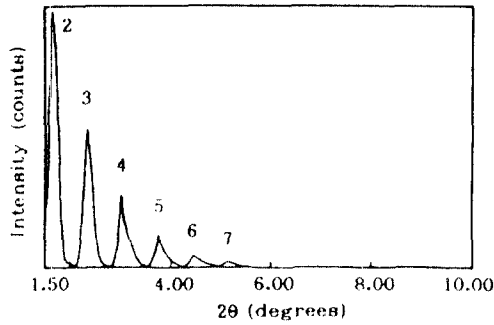


Figure 5. LXRDR pattern of Fe/TiC multilayer films with $t_{Fe}=1.2nm$, $t_{TiC}=10nm$

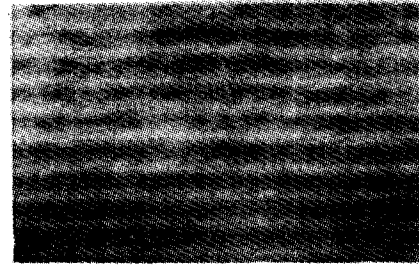


Figure 6. The multilayered structure shown by TEM with $t_{Fe}=2nm$, $t_{TiC}=4nm$

diffraction(LXRDR). Results confirmed that all these films were formed with well-defined layered structure. Fig.5 shows a LXRDR pattern of a typical sample with $t_{Fe}=1.2nm$, $t_{TiC}=10nm$. The diffraction peaks up to the seventh order can be observed, which indicates exact periodicity and sharpness of interfaces. The modulation wave length D calculated from the corrected Bragg relation^[6] was in agreement with designed values within 5%. Fig.6 shows the layered structure. The circumstance at the interface can be observed directly by HREM. A cross-section lattice image by HREM is shown in Fig.7. The sample was prepared with individual thickness $t_{Fe}=2nm$ and $t_{TiC}=4nm$. Sharp interfaces and exact periodicity are ascertained again.

3.2.2 Hardness of Fe/TiC multilayers

Most Fe/TiC multilayered films exhibited hardness higher than TiC. The hardness showed a strong dependence on the combination of individual thickness. Fig.8 shows the hardness (H_K) as a function of iron thickness while the TiC layer was kept at 8nm thick. The two dashed lines corresponding to $2300kg/mm^2$ and $200kg/mm^2$ illustrate the hardness of pure TiC and Fe film respectively. As can be seen, the hardness of the multilayers increases steadily with increasing t_{Fe} and reach a maximum of $4200kg/mm^2$ at $t_{Fe}=6nm$. Then the hardness decrease sharply with increasing t_{Fe} . The figure indicates that by adjusting the combination of individual thickness the multilayered film can achieve an much higher hardness compared to that of each constituent.

3.3 Carbon Nitride films

$\beta-C_3N_4$ is a covalent C-N solid which was predicted by material theory. It does not exist in the nature. According to the empirical model and *ab-initio* calculation of Liu and Cohen^[7], $\beta-C_3N_4$ possesses hardness and compressibility comparable to or greater than that of diamond. As a direct result of these promising characteristics, it has aroused a growing

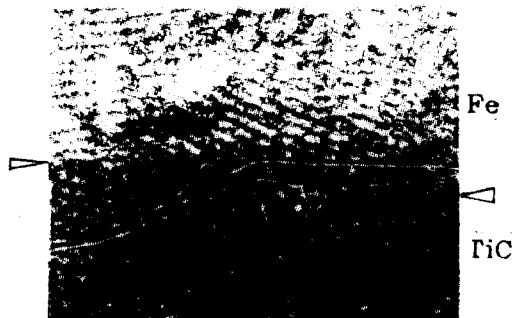


Figure 7. HREM image of interface in Fe/TiC multilayered film with $t_{Fe}=2nm$, $t_{TiC}=4nm$

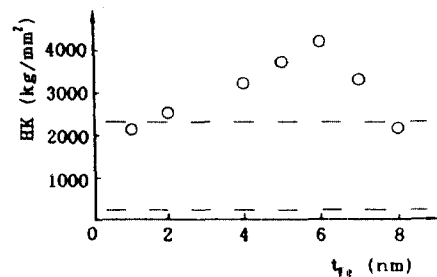


Figure 8. Knoop hardness of Fe/TiC multilayers as a function of Fe layer thickness ($t_{TiC}=8nm$)

interest in scientific research.

C-N films were synthesized in the IBA system described in section 3.2. During deposition, an ion beam of argon with current density of $3\text{mA}/\text{cm}^2$ and voltage of 3KV was exploited to sputter a pure graphite target, and another ion beam of N_2 or NH_3 was used to bombard the growing films to offer both nitrogen element and the energy of activation. The bombarding energy varied from $100\text{eV}\sim 1000\text{eV}$ and the current density varied from $0.15\sim 0.35\text{mA}/\text{cm}^2$.

3.3.1 Structure of carbon nitride film

The composition of C-N film was determined by AES. The nitrogen content was $20\sim 35\%$ for most films. The structure of C-N film was investigated by SAD of films deposited on freshly cleaved NaCl crystal. It was found that the films were composed of tiny crystallites dispersed in amorphous matrix. On the consideration of the relatively small nitrogen content, the amorphous matrix should mainly consist of excess carbon. The crystallite was identified as $\beta\text{-C}_3\text{N}_4$. Fig. 9 shows the TEM and SAD pattern of a C-N film. The film was synthesized by N^+ sputtering coupled with N^+ bombardment at 300eV and $250\mu\text{A}/\text{cm}^2$. The interplanar spacings corresponding to diffraction rings were identified as: $d_{(100)}=5.52\text{\AA}$, $d_{(210)}=2.11\text{\AA}$, $d_{(201)}=1.79\text{\AA}$, $d_{(320)}=1.27\text{\AA}$, $d_{(411)}=1.07\text{\AA}$. A good agreement with the theoretical data cited from the calculation of Niu^[7] was found. This was a direct evidence of crystalline $\beta\text{-C}_3\text{N}_4$.



Figure 9. TEM image and SAD pattern of carbon nitride film

The bonding states in C-N films was studied by XPS. Fig. 10 shows the spectra of C $1\text{S}_{1/2}$ and N $1\text{S}_{1/2}$ electrons in films synthesized under different bombardment of NH_3^{pr} . It can be seen from Fig.10(a) that C $1\text{S}_{1/2}$ peak has chemical shifts to higher bond energy. It approaches to the C $1\text{S}_{1/2}$ peak of diamond(284.5) as the bombarding energy is reduced. This reveals an increase of the C- SP^3 bondings. In Fig.10(b), the N $1\text{S}_{1/2}$ peak positions are all very close to 399.0eV , which is just the bonding energy in neutral nitrogen atom. In fact, N $1\text{S}_{1/2}$ peak in NH_3 is 405.6eV , far from that in carbon nitride film. So we can conclude that nitrogen atoms have unpolarized covalent bonds with carbon atoms.

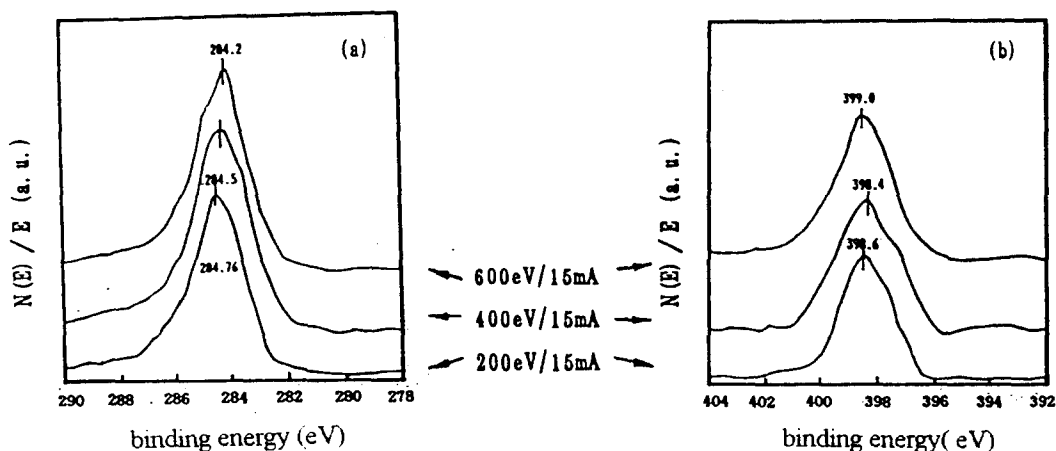


Figure 10. XPS of a) C $1\text{S}_{1/2}$ b) N $1\text{S}_{1/2}$ under various bombarding energy

3.3.4 Hardness of carbon nitride film

The hardness measurement was systematically carried out. It was found that the film hardness was sensitive to the bombarding energy. This is similar to the case of DLC, as discussed in Section 3.1.3. Nevertheless, the window energy of bombardment was slightly greater than that of DLC films. When the energy was in the range of 300~400eV, the film exhibited much higher hardness. A maximum of 5260Kg/mm² was achieved. It was also found by hardness test that the hardness was increased when the bombardment current density was increased. This is consistent with the literature^[9].

SUMMARY

In summary, we can conclude the following:

1. DLC films were synthesized by IBAD at room temperature. The films were basically amorphous, in which there were tiny diamond crystallites dispersed. Low energy bombardment can lead to abundant SP³ bonds and consequently more obvious characteristics of diamond. DLC films synthesized under 200eV bombardment showed a hardness higher than 4000Kgf/mm². They exhibited friction coefficient as low as 0.05. Even in the high load of 120N, which is close to the case of industrial bearing service, tribological performance of DLC film was much better than AISI 52100 steel.

2. Nanometer multilayered Fe/TiC films were prepared by IBAD. The multilayers showed sharp interfaces. By adjusting the combination of individual thickness, the hardness of multilayered films can be higher than that of each constituent.

3. C-N films were synthesized by IBAD at room temperature. The films consisted of tiny crystallites dispersed in amorphous matrix. The crystallites were identified as β -C₃N₄ by SAD and a good agreement with theoretical values was found. XPS study confirmed the result. The films exhibited high hardness. A maximum of 5260Kg/mm² was achieved.

References

- [1]. C. Weissmantel et al, Thin Solid Films, 72(1980)19
- [2]. A. Imamura et al, Surf. Coat. & Technol., 36(1988)161
- [3]. X.M. He et al, Tribological performance enhancement of amorphous hard carbon films on AISI 52100 steel, Surf. Coat. & Technol., 71(1995)223
- [4]. J.F. Arehard, in Wear Contral Handbook, New York, 1980, p.35
- [5]. R. Krishnan and Tessier, J. Appl. Phys. 67(1990)5391
- [6]. B.K. Agarwal, X-Ray Spectroscopy, Springer, Berlin, 1979, p.134
- [7]. Liu A.Y., Chohen L.M., Science 245(1989)841
- [8]. Niu C. et al, Science, 261(1993)334
- [9]. F. Fujumoto and K. Ogata, Jpn. J. Appl. Phys., 32(1993)L420